

Effect of PKD1 Gene Missense Mutations on Polycystin-1 Membrane Topogenesis[†]

Nancy M. Nims,[‡] Dianne Vassmer,[§] and Robin L. Maser^{*,‡,§}

[‡]*Department of Biochemistry and Molecular Biology and* [§]*Department of Clinical Laboratory Sciences, University of Kansas Medical Center, Kansas City, Kansas 66160, United States*

Received August 17, 2010; Revised Manuscript Received December 10, 2010

ABSTRACT: Polycystin-1 (PC1), the product of the polycystic kidney disease-1 (PKD1) gene, has a number of reported missense mutations whose pathogenicity is indeterminate. Previously, we utilized N-linked glycosylation reporter tags along with membrane insertion and topology assays to define the 11 membrane-spanning domains (I–XI) of PC1. In this report, we utilize glycosylation assays to determine whether two reported human polymorphisms/missense mutations within transmembrane (TM) domains VI and X affect the membrane topology of PC1. M3677T within TM VI had no effect on the topology of this TM domain as shown by the ability of two native N-linked glycosylation sites within the extracellular loop following TM VI to be glycosylated. In contrast, G4031D, within TM X, decreased the glycosylation of TM X reporter constructs, demonstrating that the substitution affected the C-terminal translocating activity of TM X. Furthermore, G4031D reduced the membrane association of TM X and XI together. These results suggest that G4031D affects the membrane insertion and topology of the C-terminal portion of polycystin-1 and represents a bona fide pathogenic mutation.

Polycystin-1 (PC1)¹ is the protein product of the PKD1 gene, which when mutated is responsible for 85% of the cases of autosomal dominant polycystic kidney disease (ADPKD). Mutations within the PKD2 gene, encoding polycystin-2 (PC2), comprise the remainder of ADPKD cases. ADPKD is a systemic disease that is primarily characterized by fluid-filled, epithelial-lined cysts within both kidneys and is associated with increased prevalence for hypertension, aneurysms, hernias, and cysts in other organs (e.g., liver and pancreas). ADPKD is highly prevalent, affecting 1 in every 500–1000 individuals, and leads to end stage renal failure in approximately half of those affected. As such, ADPKD comprises nearly 5% of the costs for renal replacement therapy in the United States (1).

PC1 is an integral plasma membrane protein that has been localized to multiple sites within the cell including the primary cilium (2–4). PC1 is composed of a large N-terminal extracellular portion, 11 transmembrane (TM) domains, and a short intracellular C-terminal tail (5, 6). The N-terminal portion of PC1 consists of multiple domains proposed to be involved in both cell–cell and cell–matrix interactions and in sensing fluid shear stress (5, 7).

The C-terminal tail interacts with multiple protein partners, is proteolytically cleaved in response to changes in mechanical stimuli, and initiates multiple signaling pathways (8–20). Evidence suggests a function for PC1 as a G protein-coupled receptor (GPCR) (21, 22), including the ability of the C-tail to directly bind heterotrimeric G proteins (10, 23). The C-tail of PC1 also interacts with PC2 via a coiled-coil domain (24). PC2 is a smaller protein with six TM domains and has been shown to form a cation-selective ion channel permeable to Ca²⁺ (25). Studies have shown an ability for PC1 and PC2 to sense fluid shear stress and initiate calcium-mediated signaling (26). Altogether, these observations suggest that PC1 is a complex, multifunctional protein capable of acting as a mechanosensor, receiving signals from the primary cilia, neighboring cells, and extracellular matrix, and transducing them across the plasma membrane to the interior of the cell.

Our previous work provided the first experimental evidence supporting an 11 TM domain (I–XI) structure for PC1 (27). Furthermore, those studies suggested that the membrane biogenesis of PC1 is somewhat complex, with TM domains I–IX inserting in a cotranslational and sequential manner, while the insertion of TM domains X and XI appeared to be noncotranslational and cooperative. Currently, nothing is known regarding how the membrane-associated structure of PC1 influences its functions or how disease-associated mutations affect the membrane topology or biogenesis of PC1. In this report, we utilize glycosylation assays of endogenous N-linked glycosylation sites or engineered glycosylation reporter gene fusions to determine whether two reported human polymorphisms/mutations within TM domains VI and X affect the membrane topology of PC1. These studies demonstrate that the disease-associated missense mutation G4031D within TM X negatively impacts the membrane-integrated structure of TM X and possibly of the last two TM domains of PC1, suggesting that it represents a pathogenic mutation.

[†]This work was supported by grants from the Polycystic Kidney Disease Foundation (Grant 98011) and the National Institute of Diabetes and Digestive and Kidney Diseases, National Institutes of Health (Grant P50-DK57301).

*To whom correspondence should be addressed: tel, (913) 945-6794; fax, (913) 588-9251; e-mail, rmaser@kumc.edu.

Abbreviations: ADPKD, autosomal dominant polycystic kidney disease; GPCR, G protein-coupled receptor; GPS, G protein-coupled receptor proteolytic cleavage site; HA, hemagglutinin; N, asparagine; N1S, single N-linked glycosylation mutant of CD5–11TM; N12S, double N-linked glycosylation mutant of CD5–11TM; N123S, triple N-linked glycosylation mutant of CD5–11TM; N3, three consensus N-linked glycosylation sites of glycosylation reporter tag; NgF, N-glycosidase F; PC1, polycystin-1; PC2, polycystin-2; PKD1, polycystic kidney disease 1 gene; PKD1L3, PKD1-like protein 3; PKD2L1, PKD2-like protein 1; PRL, prolactin; REJ, receptor for egg jelly; S, serine; SAIL, signal anchor type II; TM, transmembrane; TNT, transcription-coupled translation.

MATERIALS AND METHODS

PC1 Membrane-Associated Construct Lacking Native N-Linked Glycosylation Sites. In order to identify native, N-linked glycosylation sites within the membrane-spanning portion of PC1, three potential N-linked glycosylation sites (N3139, N3728, and N3780) within the C-terminal 1284 residues of murine polycystin-1 were sequentially removed by mutating asparagine (N) residues conforming to the N-linked consensus sequence, NxS/T, to serine (S) residues. The sites were mutated by a combination of site-directed mutagenesis (for the N3139 or N1 site; Gene Editor kit, Promega) and PCR/replacement cloning (for the N3728 or N2 and N3780 or N3 sites), as described previously (27). All mutations and the integrity of PC1 sequences were confirmed by DNA sequencing. Finally, the C-terminal 1284 residues of mutants N1S, N12S, and N123S (*ScaI*–*NotI* fragment) were joined in frame with the CD5 protein signal sequence to generate CD5–11TM^{N1S}, CD5–11TM^{N12S}, and CD5–11TM^{N123S}.

Mutant TMVI (M3677T) Expression Construct. To generate an 11 TM domain expression construct with the M3677T mutation within the sixth TM domain, CD5–11TM was used as a template for the Stratagene QuikChange kit using M3677T For (5'-AGACTCTTGGTGACACGCTTTTCTTACTGGTGA-CG-3') and M3677T Rev (5'-CGTCACCAGTAAGAAAA-GCGTGACACCAAGAGTCT-3') primers. The mutation was confirmed by DNA sequencing. In order to eliminate potential effects of offsite mutations, multiple CD5–11TM^{M3677T} clones were analyzed.

Mutant TMX (G4031D) Expression Constructs. To generate TM X mutant clones, CD5-I–X or flag-X (constructed as described (27)) were used as templates for the Stratagene QuikChange kit with G4031D For (5'-GGGAGCCACCTTGG-ACCTGGTGCTGCTTG-3') and G4031D Rev (5'-CAAG-CAGCACCAGGTCCAAGGTGGCTCCC-3') primers. Generation of the desired mutation was confirmed by DNA sequencing. Primer synthesis and DNA sequencing were performed by the staff at the Kansas Medical Center Biotechnology Support Facility.

In Vivo Expression and Glycosidase Assays. HEK293T cells were maintained in DMEM/4.5 g/L glucose/10% serum with penicillin/streptomycin. Transient transfections were performed as previously described (27). Briefly, cells were incubated with CaHPO₄–DNA precipitates consisting of 100 or 250 ng of PC1 fusion protein DNA unless otherwise noted and pBluescript (Stratagene) filler DNA for a total of 8 µg of DNA for 3.5 h. Cells were lysed 22–26 h later in passive lysis buffer (Promega). For analysis of N-linked glycosylation, lysates were supplemented with detergents at final concentrations of 1% Triton X-100, 0.5% sodium deoxycholate, and 0.1% SDS, and nuclei were pelleted. Supernatants were digested with *N*-glycosidase F (Glyko) as described previously (27). Glycosidase reactions or cell lysates were precipitated, solubilized in 2× SDS loading buffer at 65 °C, electrophoresed on either 7.5% or 5% polyacrylamide–SDS minigels, and transferred to Immobilon-P membrane (Millipore). Some blots were blocked in 5% milk–TBSN (10 mM Tris, pH 7.4, 0.9% NaCl, 0.1% NP-40) for probing with a rat anti-HA monoclonal antibody (Roche). Alternatively, for probing with antiserum raised against a C-terminal peptide of mouse PC1 (AS19 (10)), blots were blocked in 5% milk–TBST (10 mM Tris, pH 7.4, 0.9% NaCl, 0.1% Triton X-100). Blots were developed with either anti-rat HRP secondary and ECL substrate or anti-rabbit AP secondary antibody and CDP-Star and were exposed to film.

In Vitro Expression, Glycosylation, and Membrane Association Assays. For in vitro analysis of glycosylation, flag-TM-glycosylation reporter clones were incubated in coupled transcription/translation (T7 Quick TNT) extracts (Promega) with [³⁵S]methionine (Amersham) in the presence of canine pancreatic microsomes (Promega) (27). For assessment of membrane association of the flag-TM X clones, 1 µL of a TNT reaction was equilibrated in 0.5 mL of 100 mM Tris, pH 7.5, and 250 mM sucrose and then centrifuged for 30 min at 78000 rpm, 4 °C, in a TLA100.2 rotor. Resulting Tris sucrose supernatants were precipitated in methanol, dissolved in 2× SDS loading buffer, and denatured for 2 min at 100 °C. Treatment of TNT reactions with *N*-glycosidase F was in glycosylation lysis buffer (150 mM NaCl, 50 mM Tris, pH 7.5, 2 mM EDTA, 0.5% Triton X-100, 0.5% sodium deoxycholate, 0.5% SDS) (27). Following electrophoresis, gels were enhanced in 1 M sodium salicylate, dried down, and exposed to film at –70 °C.

RESULTS

TM VI Mutation M3677T Does Not Alter the Membrane Insertion or Topology of TM VI. A number of missense mutations/polymorphisms have been reported in the PKD1 gene (<http://pkdb.mayo.edu/cgi-bin/mutations.cgi>). One of these amino acid substitutions, M3677T, is located within TM VI, which has been shown to have an N_{cytosolic}–C_{extracellular} orientation (27). In order to analyze the effect of M3677T on the topology of TM VI within the context of the membrane-integrated portion of PC1, the C-terminal 1284 amino acid residues of murine PC1 were cloned with the signal sequence of CD5 protein to generate CD5–11TM (Supporting Information Figure S1A). The authenticity of three consensus, N-linked glycosylation sites within the membrane-spanning portion of PC1 was determined by a combination of mobility shift and *N*-glycosidase assays with site-directed mutants of CD5–11TM (Supporting Information Figure S1B,C). These experiments showed that the loop following TM VI contained the only native N-linked glycosylation sites within this portion of PC1 (Supporting Information Figure S1D). Therefore, the glycosylation status of this loop was used as a topology reporter to determine if the M3677T substitution affected the membrane insertion of TM VI. The M3677T mutation was engineered into CD5–11TM to generate CD5–11TM^{M3677T}, and the electrophoretic mobilities of CD5–11TM, CD5–11TM^{N123S}, and CD5–11TM^{M3677T} fusion proteins were compared (Figure 1). As observed previously (Supporting Information Figure S1B), the mobility of the wild-type and the triple glycosylation mutant CD5–11TM proteins differs considerably; however, analysis of three independent CD5–11TM^{M3677T} mutant clones showed electrophoretic mobility identical to that of wild-type CD5–11TM. These results suggest that the Met to Thr substitution at residue 3677 does not prevent TM VI from inserting into the membrane and translocating the following loop into the lumen of the ER.

TM X Mutation G4031D Decreases the Translocation Efficiency of TM X. A human disease-associated amino acid substitution, G4031D, has been reported in TM X (28). TM X was previously shown to have an N_{cytosolic}–C_{extracellular} topology (27). To determine if G4031D affects the membrane integration and C-terminal translocation of TM X *in vivo*, the amino acid substitution was engineered into the CD5-I–X glycosylation reporter clone (Figure 2A) (27). This construct contains the signal sequence of CD5 protein followed by the first 10 TM domains of PC1 and ends in the glycosylation reporter tag consisting of the

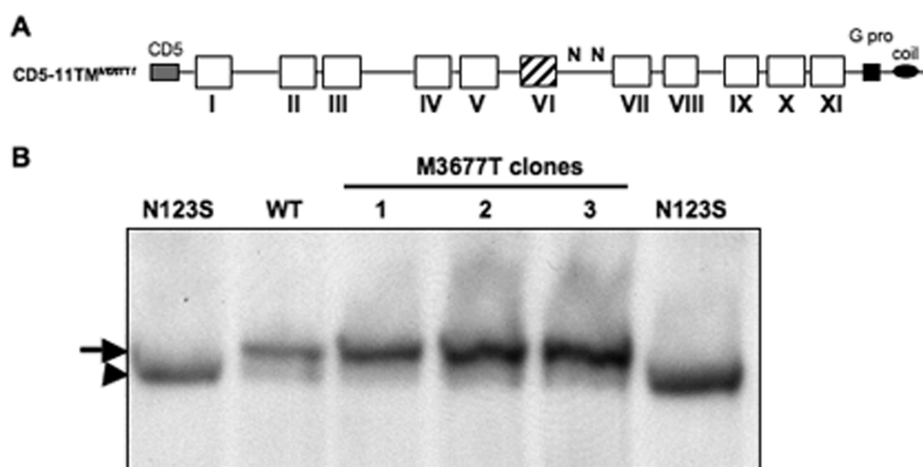


FIGURE 1: M3677T does not affect membrane integration of TM VI. (A) Illustration of the CD5–11TM^{M3677T} fusion protein with Met to Thr mutation at residue 3677 within TM VI (hatched box). Boxes and roman numerals indicate the 11 TM domains of PC1. CD5, signal sequence; G pro, G protein activation domain; coil, coiled-coil domain; N, N-linked glycosylation site. (B) AS19 Western blot analysis of lysates from 293T cells transiently transfected with CD5–11TM (WT), triple glycosylation mutant CD5–11TM^{N123S} (N123S), or three different CD5–11TM^{M3677T} mutant fusion protein clones (1–3). Arrow, glycosylated form; arrowhead, nonglycosylated form.

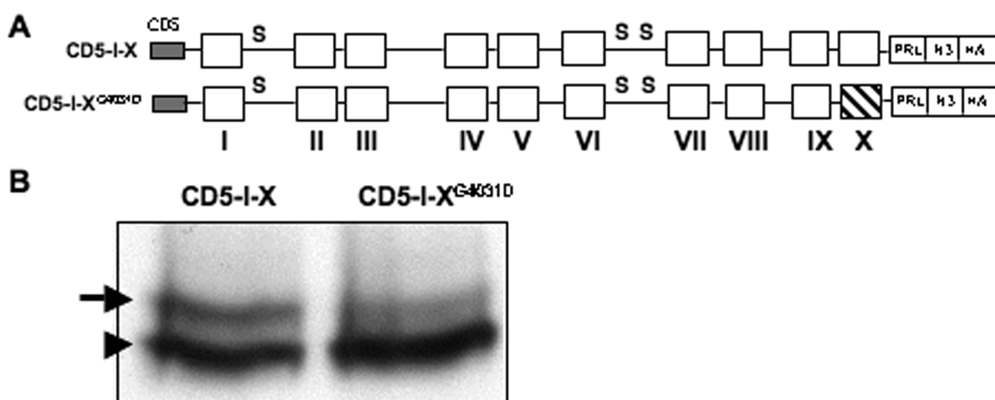


FIGURE 2: *In vivo* glycosylation analysis of TM X^{G4031D} mutant. (A) Illustration of wild-type CD5-I-X and mutant CD5-I-X^{G4031D} glycosylation reporter constructs. Both fusion proteins contain TM domains I–X of PC1 and have the three potential N-linked glycosylation sites within PC1 removed by mutation (S). CD5-I-X^{G4031D} also has the engineered Gly to Asp mutation within TM X (hatched box). CD5, signal sequence from CD5 protein; PRL-N3-HA, glycosylation reporter tag. (B) Anti-HA Western blot analysis of constructs transfected into 293T cells at a low DNA (10 ng) amount. The glycosylated (arrow) and nonglycosylated (arrowhead) forms are indicated.

topologically neutral prolactin (PRL) “spacer” sequence (29), three consensus N-linked glycosylation sites (N3), and a hemagglutinin (HA) tag (30). All native N-linked glycosylation sites were removed from PC1 sequences in order to assess glycosylation of the C-terminal glycosylation reporter tag only. The wild-type and mutant constructs were transfected into 293T cells, and their glycosylation efficiencies were analyzed by Western blot (Figure 2B). The relative proportion of glycosylated versus nonglycosylated species of wild-type CD5-I-X was less than 50% (upper band compared to lower band), which is consistent with previous results showing that TM X has somewhat weak signal anchor II activity (27). Importantly, the proportion of glycosylated to nonglycosylated species was significantly less for the CD5-I-X^{G4031D} mutant protein. These results suggest that the TM X mutant has weaker translocation activity than wild-type TM X.

To further assess the effects of the G4031D substitution, wild-type and mutant TM X domains and their N- and C-terminal loop regions were cloned in frame with an N-terminal FLAG epitope tag (flag) and the C-terminal glycosylation reporter tag (PRL-N3-HA) (Figure 3A) and were expressed in *in vitro* coupled transcription/translation (TNT) extracts in the presence of rough

microsomal membranes. Since these expression constructs lack a signal sequence, this assay reveals whether the TM domains can function to direct their own membrane-associated synthesis and integration (i.e., signal-anchor assay). Gel electrophoresis of the TNT reaction products (Figure 3B) shows that the wild-type flag-X template resulted in synthesis of both glycosylated and nonglycosylated species, as demonstrated by treatment with NgF, while the flag-X^{G4031D} template produced nonglycosylated product. Very long exposures revealed a minor amount of glycosylated flag-X^{G4031D} protein (data not shown). These *in vitro* observations are consistent with the *in vivo* data obtained with wild-type and mutant CD5-I-X fusion proteins.

G4031D Mutation Affects the Membrane Association Property of TM X. To determine whether the reduced translocation activity of the TM X mutant fusion protein is due to the loss of signal sequence properties, an aliquot of the TNT plus canine microsomal membrane reaction was centrifuged in Tris sucrose buffer, and the resulting membrane pellet (P) and supernatant (S) fractions were analyzed for amounts of fusion protein (Figure 3C). More than half of the flag-X^{G4031D} fusion protein was found in the supernatant (nonmembrane associated)

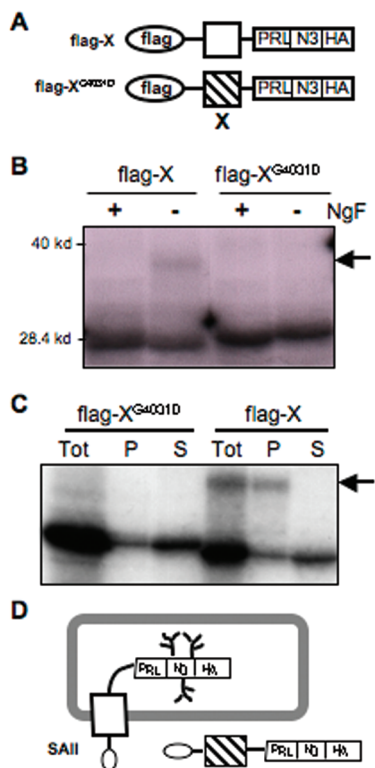


FIGURE 3: *In vitro* translocation analyses of mutant TM X. (A) Illustration of wild-type flag-X and mutant flag-X^{G4031D} glycosylation reporter tag fusion constructs. Hatched box, G4031D mutant TM domain X; flag, N-terminal FLAG epitope tag; PRL-N3-HA, glycosylation reporter tag. (B) Gel analysis of flag-X and flag-X^{G4031D} fusion proteins produced in TNT extracts with microsomal membranes and incubated with (+) or without (-) NgF. Arrow, glycosylated form. (C) Gel analysis of flag-X and flag-X^{G4031D} TNT reactions following centrifugation in Tris sucrose buffer. Both the membrane pellet (P) and supernatant (S) fractions were analyzed along with an aliquot of the total TNT reaction (Tot). Arrow, glycosylated form. (D) Interpretation of the glycosidase and membrane association studies. The location and orientation of the predominant forms of the wild-type and mutant flag-X fusion proteins are shown relative to the microsomal membrane (gray rectangle). N-linked glycosylation is illustrated by the branched structures on the N3 portion of the glycosylation reporter tag. SAIL, signal anchor II orientation.

fraction. In contrast, the majority of wild-type flag-X was present in the membrane pellet (the glycosylated and nonglycosylated forms together). This suggests that the G4031D mutation reduces the ability of TM X to act as a signal sequence and to direct its own synthesis at membrane-bound ribosomes.

G4031D Mutation May Influence the Membrane Insertion of TM X and TM XI. Previously, we showed that the membrane association and integration of TM X was increased by the addition of C-terminal sequences containing the extracellular loop and TM XI (27). To determine whether the G4031D mutation affected the ability of the two TM domains together to associate with membranes, wild-type and mutant flag-X-XI fusion proteins were synthesized in TNT extracts with microsomal membranes and subjected to centrifugation in Tris sucrose buffer. Analysis of the pellet and supernatant fractions (Figure 4B) showed that addition of TM XI resulted in approximately half of flag-X^{G4031D}-XI being associated with the microsomal membrane pellet. In contrast, the major proportion of wild-type flag-X-XI fusion protein was found in the membrane pellet. These results suggest that the G4031D mutation could

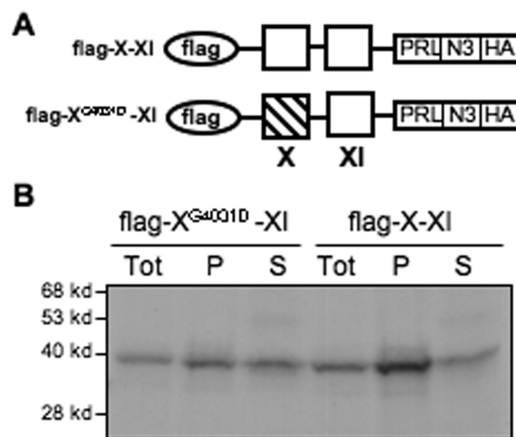


FIGURE 4: Analysis of membrane association of mutant TM X with TM XI. (A) Illustration of wild-type flag-X-XI and mutant flag-X^{G4031D}-XI glycosylation reporter tag fusion constructs. Hatched box, TM X with G4031D mutation; flag, N-terminal FLAG epitope tag; PRL-N3-HA, glycosylation reporter tag. (B) Gel analysis of flag-X-XI and flag-X^{G4031D}-XI fusion proteins produced in TNT extracts with microsomal membranes following centrifugation in Tris sucrose buffer. Both the membrane pellet (P) and supernatant (S) fractions were analyzed along with an aliquot of the total TNT reaction (Tot).

negatively impact the membrane integration of the final two TM domains of PC1.

DISCUSSION

Disease-associated mutations within the human PKD1 gene include insertions, deletions, duplications, and nonsense and missense mutations (<http://pkdb.mayo.edu/cgi-bin/mutations.cgi>). Most of the missense mutations are classified as indeterminate since the effects of these amino acid substitutions have not been and/or cannot be easily assayed. However, a few PKD1 missense mutations have been demonstrated to impact properties and functions described for PC1. PKD1 family related mutations within the receptor for egg jelly (REJ) domain were shown to prevent cleavage at the GPS domain, to abolish STAT1 activation, and to prevent *in vitro* tubulogenesis (31). Several missense mutations within the first PKD repeat were shown to alter the stability of the folding of this domain, which was proposed to affect its function in mechanosensing (7, 32). A missense mutation within the coiled-coil domain of the cytosolic C-terminal tail of PC1 was found to alter its ability to interact with, activate, and stabilize PC2 (33–35). Currently, nothing is known regarding how human disease-associated mutations affect the membrane topology or biogenesis of PC1. The Pkd1^{m1Be1} mouse is the only known example of a missense mutation within a TM domain of PC1 that leads to cystic disease (36). In this instance, ENU mutagenesis generated a Met to Arg substitution (M3083R) within TM domain I which resulted in a mouse model with a homozygous null phenotype. The molecular basis by which M3083R leads to the complete loss of PC1 function is not known, however. Previously, we developed expression constructs and assays that enabled us to determine the location and topology of the 11 TM domains and intervening loop regions of PC1 (27). In this report, we utilize electrophoretic mobility shift, glycosidase, and membrane association assays to determine whether two reported human missense mutations within TM domains VI and X affect the membrane-associated structure of PC1.

Glycosidase and mobility shift assays with single, double, and triple glycosylation mutants were used to demonstrate the

presence of two, native N-linked glycosylation sites within the CD5–11TM expression construct of PC1. The results of these assays (Supporting Information Figure S1D) are consistent with the experimentally supported membrane topology model for PC1 (27). Both N2 (N3728), and N3 (N3780) glycosylation sites are located in the extracellular loop after TM VI where they would be exposed to modifying enzymes during synthesis of the protein in the ER. In contrast, N1 (N3139) is located within the first intracellular loop and, therefore, would not be expected to be glycosylated. Furthermore, the sequence for N1 is NPT, and there are reports that “x”, in the N-linked glycosylation consensus sequence, NxS/T, can be any amino acid residue except proline (37). Confirmation of the authenticity of N2 and N3 as glycosylation sites allowed them to be used as topology reporters for a missense mutation in TM VI (see below). It is anticipated that these N-linked glycosylation sites will be useful for assaying the effects of other missense mutations within preceding TM domains (e.g., TM I–V) or within other regions of PC1 that might impact its topology and/or transport from the ER (i.e., by Endo H cleavage resistance-susceptibility assays).

One of the ADPKD-associated amino acid substitutions investigated was M3677T, located in TM domain VI. M3677T did not alter the electrophoretic mobility of CD5–11TM (Figure 1), indicating that sites N2 and N3 were glycosylated as in wild-type CD5–11TM (Supporting Information Figure S1). The ability of sites N2 and N3 to be glycosylated suggests that this amino acid substitution did not alter the membrane insertion or orientation of TM VI. However, this approach is unable to discern if M3677T causes a more subtle change such as a shifting in the location of the membrane-embedded residues of TM domain VI. It is possible that M3677T may affect other properties of PC1 such as its stability or the ability of TM VI to interact with other TM domains of PC1 or with interacting partners such as PC2. Recently, the TM domain portions of PC1- and PC2-related proteins PKD1L3 and PKD2L1 were shown to interact with each other in order for this complex to be transported to taste pores (38). Although the stability of the M3677T mutant of CD5–11TM did not appear to be altered (as compared to wild-type CD5–11TM) in our studies, we realize that ours represents an overexpression system that might overwhelm endogenous degradative mechanisms. Finally, it is also possible that M3677T represents a harmless polymorphism based on the observation that although Met is present at residue 3677 in PC1 from human, mouse, rat, dog, and chicken, the corresponding residue in *Fugu* PC1 is Thr.

The second ADPKD-associated missense mutation investigated was G4031D, located within TM domain X. Previous work demonstrated that TM X has the ability, albeit weak, to translocate its C-terminus and associated sequences into the ER lumen (i.e., signal anchor type II or SAII activity) (27). Assays with glycosylation reporter fusion proteins expressed either *in vivo* or *in vitro* showed that mutant TM X was less efficiently glycosylated than wild-type TM X-containing proteins, suggesting that the G4031D mutation interferes with the SAII activity of TM X (Figures 2 and 3). In addition, previous work had shown that the addition of TM XI and intervening loop sequences to TM X significantly increased the membrane association of TM X. This was interpreted to suggest that the membrane integration of TM X requires multiple topogenic determinants and occurs via a cooperative mechanism involving TM XI (27). To determine whether the G4031D mutation affected this cooperative phenotype, loop-TM XI sequences were added to mutant TM X.

Addition of TM XI only slightly improved the membrane association of mutant TM X, in contrast to its significantly positive effect on the membrane association of wild-type TM X (Figure 4). Thus, the G4031D mutation not only reduces the membrane association and translocation of TM X alone but also diminishes the membrane association of the last two TM domains together.

Predictive algorithms represent an alternative method to the experimental testing of the effect of a missense mutation on the topology of a transmembrane domain. Using the Phobius (www.ebi.ac.uk/Tools/phobius/) and TMHMM (www.cbs.dtu.dk/services/TMHMM-2.0/) protein topology prediction programs, neither the G4031D nor the M3677T variant is predicted to eliminate or to alter the topology of its respective TM domain (data not shown). For G4031D, however, the probability for residues within the domain to be membrane-embedded is reduced, and there is a suggestion that the membrane-spanning portion may be shifted C-terminal-ward and shortened. In addition, the probabilities for the preceding and following loops to be located inside and outside of the cell, respectively, are less definitive with G4031D than with G4031. Any apparent discrepancy between experimental and predictive results may be due to their inherent strengths and weaknesses. For example, although our glycosylation reporter approach involves the overexpression, or the *in vitro* expression, of artificial, truncated PC1 constructs, it is a valid method to biochemically assess the membrane association and topology of a predicted TM domain. While topology prediction programs are invaluable bioinformatic tools, it is important to recognize that it is experimentally derived structural data (e.g., from NMR, X-ray crystallography, gene fusions, cysteine substitution, N-linked glycosylation, and protease protection assays) that are used as training sets for developing these algorithms and that are also used as test sets to determine the accuracy of the program. Currently, there is no topology prediction program that is 100% accurate (39). Some of this inaccuracy stems from an inability to factor in the influence of one domain upon another, the distances between TM domains, the regulation of translocation by other factors, and the amphipathic nature of TM domains internal to the protein.

The data in this report support the view that G4031D would interfere with the membrane insertion of TM X and TM XI *in vivo* and thereby represents a pathogenic mutation. Several possibilities exist as to what the molecular pathogenic effects of G4031D could be. For example, inhibition of the membrane integration of TM X and TM XI would result in the cytosolic localization of these TM domains and intervening loop sequences and could alter the structure or environment of the cytosolic C-tail, potentially influencing its cleavage and disrupting the multiple signaling functions ascribed to this portion of PC1 (10, 13–19). Furthermore, the cytoplasmic exposure of sequences normally embedded within the membrane might lead to gratuitous activation of nonspecific signaling effectors, resulting in a dominant gain of function. An intriguing idea is that the membrane integration of (wild type) TM X and XI may be “purposefully” inefficient and/or regulated (40). In this scenario, alternative, membrane-integrated conformations of PC1, consisting of 11 or 9 TM forms, each with different signaling properties, could be synthesized at the ER. G4031D would favor the predominance of the 9 TM conformation and its signaling activities, which could result in a pathological imbalance in the pathways activated. The L envelope protein of the hepatitis B virus is an example of a protein with dual membrane-integrated

structures that are linked to different functions and whose biogenesis is regulated (41). Alternatively, G4031D might interfere with an entirely different biochemical property of TM X, such as its ability to interact with other TM domains. With regard to this, we have noticed that G4031D disrupts a potential GxxxG motif at the N-terminal end of TM X. GxxxG motifs are important for transmembrane domain packing and oligomerization of many types of integral membrane proteins, including GPCRs (42–44). Interestingly, the GxxxG motif is conserved in TM X of human, rat, mouse, and dog PC1 and is replaced by the GxxxG-like motif (44, 45), AxxxA, in chicken and *Fugu* PC1.

In summary, our studies provide biochemical evidence that is highly supportive of a pathological, rather than a neutral, effect of G4031D. Currently, we are unable to conclude whether G4031D represents an inactivating or a hypomorphic mutation. These data warrant future studies that will determine whether this amino acid substitution affects the biological properties of PC1 (e.g., cellular localization, signaling, and tubulogenesis) and leads to a disease phenotype.

ACKNOWLEDGMENT

We gratefully acknowledge the assistance of Brenda S. Magenheimer. The investigators are members of the Kansas Interdisciplinary Center for PKD Research. In memory of Nancy M. Nims.

SUPPORTING INFORMATION AVAILABLE

N-linked glycosylation sites within the membrane spanning portion of polycystin-1 as determined by site-directed mutagenesis and *N*-glycosidase analysis. This material is available free of charge via the Internet at <http://pubs.acs.org>.

REFERENCES

- Harris, P. C., and Torres, V. E. (2009) Polycystic kidney disease. *Annu. Rev. Med.* 60, 321–337.
- Wilson, P., Geng, L., Li, X., and Burrow, C. (1999) The PKD1 gene product, “polycystin-1”, is a tyrosine-phosphorylated protein that colocalizes with α 2 β 1-integrin in focal clusters in adherent renal epithelia. *Lab. Invest.* 79, 1311–1323.
- Scheffers, M. S., van der Bent, P., Prins, F., Spruit, L., Breuning, M. H., Litvinov, S. V., de Heer, E., and Peters, D. J. (2000) Polycystin-1, the product of the polycystic kidney disease 1 gene, co-localizes with desmosomes in MDCK cells. *Hum. Mol. Genet.* 9, 2743–2750.
- Yoder, B., Hou, X., and Guay-Woodford, L. (2002) The polycystic kidney disease proteins, polycystin-1, polycystin-2, polaris, and cystin, are co-localized in renal cilia. *J. Am. Soc. Nephrol.* 13, 2508–2516.
- Hughes, J., Ward, C., Peral, B., Aspinwall, R., Clark, K., San Millan, J., Gamble, V., and Harris, P. (1995) The polycystic kidney disease 1 (PKD1) gene encodes a novel protein with multiple cell recognition domains. *Nat. Genet.* 10, 151–160.
- Sandford, R., Sgotto, B., Aparicio, S., Brenner, S., Vaudin, M., Wilson, R., Chissole, S., Pepin, K., Bateman, A., Chothia, C., Hughes, J., and Harris, P. (1997) Comparative analysis of the polycystic kidney disease 1 (PKD1) gene reveals an integral membrane glycoprotein with multiple evolutionary conserved domains. *Hum. Mol. Genet.* 6, 1483–1489.
- Forman, J. R., Qamar, S., Paci, E., Sandford, R. N., and Clarke, J. (2005) The remarkable mechanical strength of polycystin-1 supports a direct role in mechanotransduction. *J. Mol. Biol.* 349, 861–871.
- Huan, Y., and van Adelsberg, J. (1999) Polycystin-1, the PKD1 gene product, is in a complex containing E-cadherin and the catenins. *J. Clin. Invest.* 104, 1459–1468.
- Xu, G. M., Sikaneta, T., Sullivan, B. M., Zhang, Q., Andreucci, M., Stehle, T., Drummond, I., and Arnaout, M. A. (2001) Polycystin-1 interacts with intermediate filaments. *J. Biol. Chem.* 276, 46544–46552.
- Parnell, S., Magenheimer, B., Maser, R., Rankin, C., Smine, A., Okamoto, T., and Calvet, J. (1998) The polycystic kidney disease-1 protein, polycystin-1, binds and activates heterotrimeric G-proteins in vitro. *Biochem. Biophys. Res. Commun.* 251, 625–631.
- Puri, S., Magenheimer, B., Maser, R., Ryan, E., Zien, C., Walker, D., Wallace, D., Hempson, S., and Calvet, J. (2004) Polycystin-1 activates the calcineurin/NFAT (nuclear factor of activated T-cells) signaling pathway. *J. Biol. Chem.* 279, 55455–55464.
- Xiao, Z., Zhang, S., Magenheimer, B. S., Luo, J., and Quarles, L. D. (2008) Polycystin-1 regulates skeletogenesis through stimulation of the osteoblast-specific transcription factor RUNX2-II. *J. Biol. Chem.* 283, 12624–12634.
- Kim, E., Arnould, T., Sellin, L. K., Benzing, T., Fan, M. J., Gruning, W., Sokol, S. Y., Drummond, I., and Walz, G. (1999) The polycystic kidney disease 1 gene product modulates Wnt signaling. *J. Biol. Chem.* 274, 4947–4953.
- Arnould, T., Kim, E., Tsiokas, L., Jochimsen, F., Gruning, W., Chang, J. D., and Walz, G. (1998) The polycystic kidney disease 1 gene product mediates protein kinase C α -dependent and c-Jun N-terminal kinase-dependent activation of the transcription factor AP-1. *J. Biol. Chem.* 273, 6013–6018.
- Bhunia, A., Piontek, K., Boletta, A., Liu, L., Qian, F., Xu, P., Germino, F., and Germino, G. (2002) PKD1 induces p21(waf1) and regulation of the cell cycle via direct activation of the JAK-STAT signaling pathway in a process requiring PKD2. *Cell* 109, 157–168.
- Low, S. H., Vasanth, S., Larson, C. H., Mukherjee, S., Sharma, N., Kinter, M. T., Kane, M. E., Obara, T., and Weimbs, T. (2006) Polycystin-1, STAT6, and P100 function in a pathway that transduces ciliary mechanosensation and is activated in polycystic kidney disease. *Dev. Cell* 10, 57–69.
- Dere, R., Wilson, P. D., Sandford, R. N., and Walker, C. L. (2010) Carboxy terminal tail of polycystin-1 regulates localization of TSC2 to repress mTOR. *PLoS One* 5, e9239.
- Lal, M., Song, X., Pluznick, J. L., Di Giovanni, V., Merrick, D. M., Rosenblum, N. D., Chauvet, V., Gottardi, C. J., Pei, Y., and Caplan, M. J. (2008) Polycystin-1 C-terminal tail associates with beta-catenin and inhibits canonical Wnt signaling. *Hum. Mol. Genet.* 17, 3105–3117.
- Li, Y., Santoso, N. G., Yu, S., Woodward, O. M., Qian, F., and Guggino, W. B. (2009) Polycystin-1 interacts with inositol 1,4,5-trisphosphate receptor to modulate intracellular Ca^{2+} signaling with implications for polycystic kidney disease. *J. Biol. Chem.* 284, 36431–36441.
- Chauvet, V., Tian, X., Husson, H., Grimm, D., Wang, T., Hiesberger, T., Igarashi, P., Bennett, A., Ibraghimov-Beskrovnaya, O., Somlo, S., and Caplan, M. (2004) Mechanical stimuli induce cleavage and nuclear translocation of the polycystin-1 C terminus. *J. Clin. Invest.* 114, 1433–1443.
- Parnell, S., Magenheimer, B., Maser, R., Zien, C., Frischauf, A., and Calvet, J. (2002) Polycystin-1 activation of c-Jun N-terminal kinase and AP-1 is mediated by heterotrimeric G proteins. *J. Biol. Chem.* 277, 19566–19572.
- Delmas, P., Nomura, H., Li, X., Lakkis, M., Luo, Y., Segal, Y., Fernandez-Fernandez, J., Harris, P., Frischauf, A., Brown, D., and Zhou, J. (2002) Constitutive activation of G-proteins by polycystin-1 is antagonized by polycystin-2. *J. Biol. Chem.* 277, 11276–11283.
- Yuasa, T., Takakura, A., Denker, B., Venugopal, B., and Zhou, J. (2004) Polycystin-1L2 is a novel G-protein-binding protein. *Genomics* 84, 126–138.
- Qian, F., Germino, F. J., Cai, Y., Zhang, X., Somlo, S., and Germino, G. G. (1997) PKD1 interacts with PKD2 through a probable coiled-coil domain. *Nat. Genet.* 16, 179–183.
- Gonzalez-Perret, S., Kim, K., Ibarra, C., Damiano, A., Zotta, E., Batelli, M., Harris, P., Reisin, I., Arnaout, M., and Cantiello, H. (2001) Polycystin-2, the protein mutated in autosomal dominant polycystic kidney disease (ADPKD), is a Ca^{2+} -permeable nonselective cation channel. *Proc. Natl. Acad. Sci. U.S.A.* 98, 1182–1187.
- Nauli, S., Alenghat, F., Luo, Y., Williams, E., Vassilev, P., Li, X., Elia, A., Lu, W., Brown, E., Quinn, S., Ingber, D., and Zhou, J. (2003) Polycystins 1 and 2 mediate mechanosensation in the primary cilium of kidney cells. *Nat. Genet.* 33, 129–137.
- Nims, N., Vassmer, D., and Maser, R. (2003) Transmembrane domain analysis of polycystin-1, the product of the polycystic kidney disease-1 (PKD1) gene: evidence for 11 membrane-spanning domains. *Biochemistry* 42, 13035–13048.
- Daniels, C., Maheshwar, M., Lazarou, L., Davies, F., Coles, G., and Ravine, D. (1998) Novel and recurrent mutations in the PKD1 (polycystic kidney disease) gene. *Hum. Genet.* 102, 216–220.
- Rothman, R. E., Andrews, D. W., Calayag, M. C., and Lingappa, V. R. (1988) Construction of defined polytopic integral transmembrane proteins. The role of signal and stop transfer sequence permutations. *J. Biol. Chem.* 263, 10470–10480.

30. Lehmann, S., Chiesa, R., and Harris, D. A. (1997) Evidence for a six-transmembrane domain structure of presenilin 1. *J. Biol. Chem.* 272, 12047–12051.
31. Qian, F., Boletta, A., Bhunia, A., Xu, H., Liu, L., Ahrabi, A., Watnick, T., Zhou, F., and Germino, G. (2002) Cleavage of polycystin-1 requires the receptor for egg jelly domain and is disrupted by human autosomal-dominant polycystic kidney disease 1-associated mutations. *Proc. Natl. Acad. Sci. U.S.A.* 99, 16981–16986.
32. Ma, L., Xu, M., Forman, J. R., Clarke, J., and Oberhauser, A. F. (2009) Naturally occurring mutations alter the stability of polycystin-1 polycystic kidney disease (PKD) domains. *J. Biol. Chem.* 284, 32942–32949.
33. Casuscelli, J., Schmidt, S., DeGray, B., Petri, E. T., Celic, A., Foltá-Stogniew, E., Ehrlich, B. E., and Boggan, T. J. (2009) Analysis of the cytoplasmic interaction between polycystin-1 and polycystin-2. *Am. J. Physiol. Renal Physiol.* 297, F1310–F1315.
34. Xu, G., Gonzalez-Perrett, S., Essafi, M., Timpanaro, G., Montalbetti, N., Arnaout, M., and Cantiello, H. (2003) Polycystin-1 activates and stabilizes the polycystin-2 channel. *J. Biol. Chem.* 278, 1457–1462.
35. Vandrope, D., Wilhelm, S., Jiang, L., Ibragimov-Beskrovnaya, O., Chernova, M., Stuart-Tilley, A., and Alper, S. (2002) Cation channel regulation by COOH-terminal cytoplasmic tail of polycystin-1: mutational and functional analysis. *Physiol. Genomics* 28, 87–98.
36. Herron, B. J., Lu, W., Rao, C., Liu, S., Peters, H., Bronson, R. T., Justice, M. J., McDonald, J. D., and Beier, D. R. (2002) Efficient generation and mapping of recessive developmental mutations using ENU mutagenesis. *Nat. Genet.* 30, 185–189.
37. Marshall, R. D. (1972) Glycoproteins. *Annu. Rev. Biochem.* 41, 673–702.
38. Ishimaru, Y., Katano, Y., Yamamoto, K., Akiba, M., Misaka, T., Roberts, R. W., Asakura, T., Matsunami, H., and Abe, K. (2010) Interaction between PKD1L3 and PKD2L1 through their transmembrane domains is required for localization of PKD2L1 at taste pores in taste cells of circumvallate and foliate papillae. *FASEB J.* 24, 4058–4067.
39. Hu, J., and Yan, C. (2008) HMM_RA: an improved method for alpha-helical transmembrane protein topology prediction. *Bioinform. Biol. Insights* 2, 67–74.
40. Hedge, R. S., and Kang, S. W. (2008) The concept of translocational regulation. *J. Cell Biol.* 182, 225–232.
41. Lambert, C., and Prange, R. (2003) Chaperone action in the post-translational topological reorientation of the hepatitis B virus large envelope protein: implications for translocational regulation. *Proc. Natl. Acad. Sci. U.S.A.* 100, 5199–5204.
42. Overton, M. C., Chinault, S. L., and Blumer, K. J. (2003) Oligomerization, biogenesis, and signaling is promoted by a glycoporphin A-like dimerization motif in transmembrane domain 1 of a yeast G protein-coupled receptor. *J. Biol. Chem.* 278, 49369–49377.
43. Russ, W. P., and Engelman, D. M. (2000) The GxxxG motif: a framework for transmembrane helix-helix association. *J. Mol. Biol.* 296, 911–919.
44. Senes, A., Engel, D. E., and DeGrado, W. F. (2004) Folding of helical membrane proteins: the role of polar, GxxxG-like and proline motifs. *Curr. Opin. Struct. Biol.* 14, 465–479.
45. Kleiger, G., Grothe, R., Mallick, P., and Eisenberg, D. (2002) GXXXG and AXXXA: common alpha-helical interaction motifs in proteins, particularly in extremophiles. *Biochemistry* 41, 5990–5997.